Analysis of Upper Bound Power Output for a Wrist-Worn Rotational Energy Harvester from Real-World Measured Inputs

2014 J. Phys.: Conf. Ser. 557 012090

(http://iopscience.iop.org/1742-6596/557/1/012090)

Analysis of Upper Bound Power Output for a Wrist-Worn Rotational Energy Harvester from Real-World Measured Inputs

T Xue[1], X Ma[2], C Rahn[2] and S Roundy[1]

[1] University of Utah, Department of Mechanical Engineering, 50 S. Central Campus Drive, Salt Lake City, UT, USA
[2] Pennsylvania State University, Department of Mechanical and Nuclear Engineering, University Park, PA, USA

E-mail: tiancheng.xue@utah.edu

Abstract. Energy harvesting from human motion addresses the growing need for battery-free health and wellness sensors in wearable applications. The major obstacles to harvesting energy in such applications are low and random frequencies due to the nature of human motion. This paper presents a generalized rotational harvester model in 3 dimensions to determine the upper bound of power output from real world measured data. Simulation results indicate much space for improvement on power generation comparing to existing devices. We have developed a rotational energy harvester for human motion that attempts to close the gap between theoretical possibility and demonstrated devices. Like previous work, it makes use of magnetically plucked piezoelectric beams. However, it more fully utilizes the space available and has many degrees of freedom available for optimization. Finally we present a prototype harvester based on the coupled harvester model with preliminary experimental validation.

1. Introduction

Energy harvesting has been a promising solution as the alternative to traditional systems powered by batteries when energy independence is required. As the power consumption becomes a major obstacle to the emerging market for wearable technologies, kinetic energy contained in human daily activities naturally appeals to the researchers in the field of energy harvesting. Due to the low and random frequencies of human motion, which usually occurs around 1 Hz [1], resonant harvesters cannot benefit from the peak dynamic magnification. The well-known Seiko Kinetic watch converts the kinetic energy of a rotor to electricity using an electromagnetic generator [2]. Such rotational designs with non-resonant configuration are the common approaches that researchers have adopted to overcome the limitation of conventional linear harvesters. While the Seiko Kinetic watch boosts its energy density by a sophisticated high-ratio gear train, another strategy, which is often referred to as frequency up-conversion, is to excite a higher-frequency resonance in a transducer via a slower-frequency motion. Prior reported non-resonant harvesters include a piezoelectric harvester with in-plane magnetic plucking based on a planar rotor model [3] and a magnetic spherical harvester [4].

The goal of this paper is to provide an estimate of the maximum power output from a rotational harvester regardless of the energy conversion mechanism using real-world measured data such as

walking and jogging as inputs. We derived a generalized 3D rotor model to fulfil the task. Simulation results show that the upper bound on power generation from an eccentric rotor during normal activities is approximately an order of magnitude greater than what has been demonstrated [3], which motivates us to develop an optimized non-resonant piezoelectric harvester with different magnet-beam configurations from previous designs in the literature. We use multiple piezoelectric beams and magnets in alternate configurations that allow us to optimize the system electromechanical coupling and provide more design variables to tune the system dynamics.

2. Generalized Rotational Harvester Modelling

2.1. Generalized Rotor Model in 3 Dimensions

In order to provide an estimate of the maximum possible power generation from real-world multidimensional inputs, a full rotor model in 3 dimensions is required. The planar rotor model described in [5] only accounted for one rotational or linear excitation separately. We extended this model to 3 dimensions with 6 effective inputs simultaneously as illustrated in Figure 1. An electrical and a mechanical rotational damper are included in the model to represent extracted and lost energy respectively. The electrical damper represents any kind of ideal energy transducer while the mechanical damper represents a combined pathway for all kinds of energy losses (e.g. friction). As in many previous published studies [6, 7], this model makes the assumption that the power dissipated through an optimal viscous damper that represents the electromechanical transducer is the maximum electrical power that can be extracted from the system. The rotation of the rotor is constrained in the XY plane and the governing equations of the rotor motion are given by:

$$m\begin{bmatrix} -l\cos\phi_z\cdot\dot{\phi}_z^2 - l\sin\phi_z\cdot\ddot{\phi}_z \\ -l\sin\phi_z\cdot\dot{\phi}_z^2 + l\cos\phi_z\cdot\ddot{\phi}_z \end{bmatrix} = -m\begin{bmatrix} \ddot{X} \\ \ddot{Y} \end{bmatrix} + \begin{bmatrix} F_x \\ F_y \end{bmatrix} + m\begin{bmatrix} g_x \\ g_y \end{bmatrix} \tag{1}$$

$$I_G\left(\ddot{\theta}_z + \ddot{\phi}_z\right) = -\left(D_e + D_m\right)\dot{\phi}_z + F_x l\sin\phi_z - F_y l\cos\phi_z \tag{2}$$

Where m, I_G, and l are the mass, the moment of inertia and the eccentric distance of the rotor respectively. $\ddot{X}$, $\ddot{Y}$ are acceleration inputs to the system. F_x, F_y and g_x, g_y are the forces from the housing and gravity acting on the rotor respectively in each local coordinate. ϕ_z denotes the relative angular displacement between the rotor and the housing, which determines the power output as:

$$P = D_e\dot{\phi}_z^2 \tag{3}$$

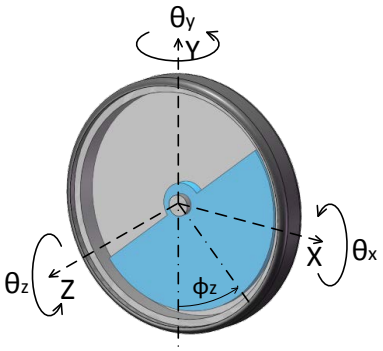

Figure 1. Dynamic model of eccentric rotor. θ_x, θ_y and θ_z denote rotational inputs to the housing while there are linear accelerations in X, Y and Z coordinates as well

2.2. Simulation with Real-World Measured Data

The input data was measured using the TEMPO Inertial BSN Platform [8], which captures motion in full six degrees of freedom. One subject wearing the platform on his wrists was instructed to

conduct a series of activities involving wrist motion including walking, jogging, running, typing, and reading. Gravitational force in X-Y plane is determined by the orientation calculated using the gyroscope data. Given certain real-world input, the power output was found to be a function of the electrical damping coefficient and rotor size when the mechanical damping coefficient was held constant. Simulation results, given in Figure 2, show that a generalized harvester placed on the wrist of a walking subject can provide an average power of 110 μW for a brass rotor of 16mm in radius and 3mm in thickness with reasonable friction. An optimal level of electrical damping is required to achieve the maximum power output. It is also obvious that the system generates more power with a lower mechanical damping level.

Figure 3 details the upper bound on power output from the generalized harvester in common daily activities. Typing produces very low power as it involves little wrist movement whereas there is a large amount of potential power in intense activities such as running and jogging. Reading and walking provide similar amounts of power as they are both mild activities involving some back-and-forth wrist motion. This generalized model provides an estimate of maximum power generation in an ideal scenario in which the electromechanical coupling can be closely approximated by an optimal linear viscous damper and parasitic electrical losses are neglected. In more specified cases, certain constraints will lower the maximum power output.

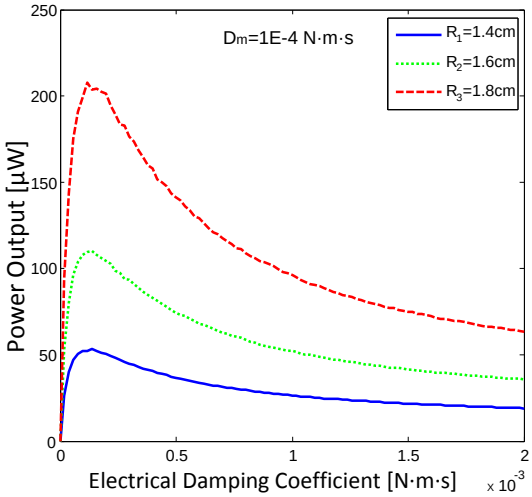

Figure 2. Power output vs. Electrical damping coefficient from the generalized rotational harvester during walking

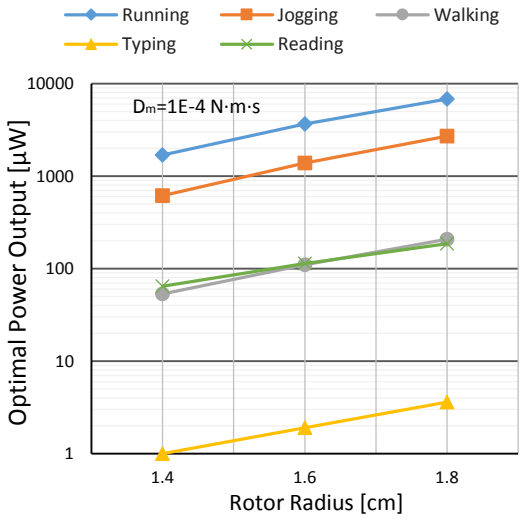

Figure 3. Upper bound on power generation from the generalized rotational harvester in different activities

3. Piezoelectric Rotational Harvester Design

We adopted the out-of-plane beam deflection configuration (i.e. the beam deflects out of the X-Y plane defined in Figure 1 rather than in the X-Y plane) in the design due to its potential for multiple beams and the simplicity of manufacture. As illustrated in Figure 4, the harvester uses repulsive magnets to achieve the actuation with magnets embedded in the rotor and on the tip of the beams. A 6-cantilever-beam array is attached on the lid to fully utilize the space within the device. Energy conversion is achieved by piezoelectric beams as three of them vibrate synchronously while the semi-circular rotor swings. Figure 5 shows a photo of the prototype harvester made with off-the-shelf piezoelectric beams and magnets. The 15-mm-radius rotor is built with slots for variable magnet spacing. We attached only one 0.38-mm-thick bimorph beam, manufactured by Piezo Systems, on the plate for the initial test. Its active length was shortened to 10 mm to fit in the device. With an NdFeB

magnet (1/16 inch^3, grade N52) on its tip, the resonant frequency of the beam is around 1000 Hz. The effective volume of the prototype inside the housing is 6 cm^3 while the total device weights 27 g with only one assembled beam and one pair of magnets attached.

In order to model this system, the equations in (1) and (2) above need to be augmented with a piezoelectric bimorph beam model and a magnetic interaction model. Many researchers have developed different approaches to formulate mathematical models for the piezoelectric harvesters. The beam model adopted in this work is based on the distributed parameter model presented in [9]. A similar modelling procedure is described in [10]. The model is altered as the excitation is the magnetic force on the tip instead of the base of the beam. The magnetic interaction force is approximated for simplicity using a magnetic dipole model, which predicts a steeper force gradient than the more accurate finite element model. We derived such a coupled rotor-magnet-beam model with multiple design variables for future optimization.

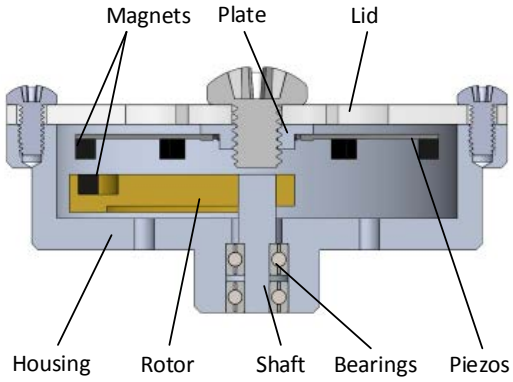

Figure 4. Piezoelectric rotational harvester CAD model (with 6 beams) in section view

Figure 5. Photo of the piezoelectric rotational harvester prototype (with one beam)

4. Experiment

4.1. Experimental Set Up

We developed the experimental set up shown in Figure 6 to test the harvester in a pseudo wrist-worn situation. The current configuration is to test motions in the vertical plane, however the servo can be mounted with different configurations. The one-beam prototype harvester is attached to the swing arm controlled by the servo. Since the definition of certain human motion is vague and subjective, by varying the swing profile (angle, speed and harvester location on the swing arm), we created a series of pseudo human motion from gentle to relatively intense walking for qualitative comparison with simulation results of the coupled harvester model. Voltage output was measured from a resistive load of 100kΩ as a match to simulation.

4.2. Experimental Results

Figure 7 shows the average power harvested from one piezoelectric beam in the test while simulation results indicate a power output ranging from 0.8 to 4 μW with high degrees of dependency on initial conditions. Simulation with a very gentle real-world walking motion also demonstrates power output above 1 μW. Preliminary test results show that power generation benefits from higher swing radius and higher frequency. (Note, that for a given angular velocity, a 60 degree rotation will have a higher frequency than a 120 degree rotation.) The one-beam harvester can generate an average power output of 3.8 μW in a relatively intense pseudo walking motion. With the possibility of 6 beams embedded, the simulation model suggests that the total power output will be at least 3 times the power generated by one beam. Due to the high resonant frequency of the shortened off-the-shelf beam, the

ring down phenomena of the plucking is not clearly demonstrated in the walking motion. Performance improvement can be achieved with a softer custom made piezoelectric beam.

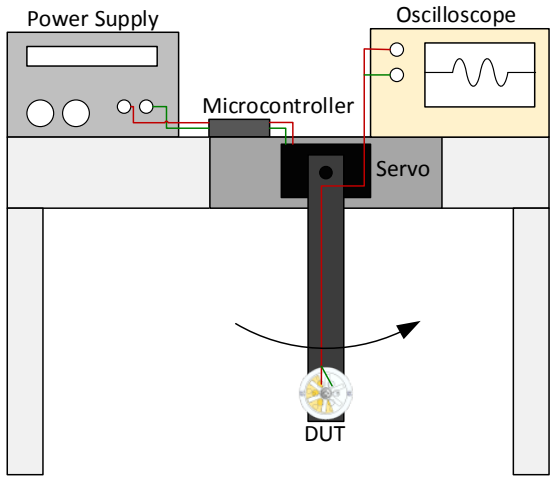

Figure 6. Experimental set-up for testing the one-beam prototype in the swing motion

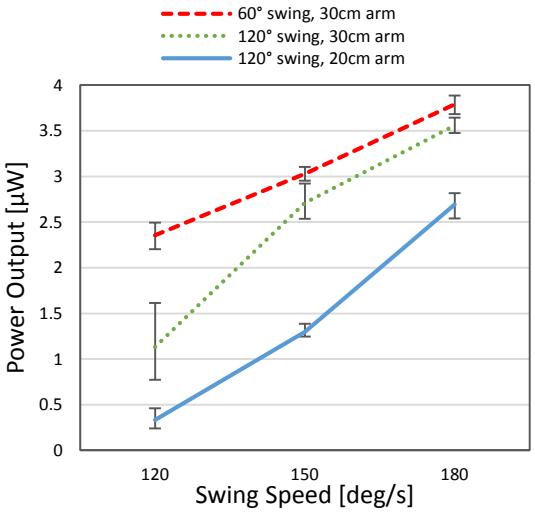

Figure 7. Average power output from pseudo walking motions

5. Conclusions

This paper presents a generalized 3D rotational harvester model to provide an estimate on maximum power output from wrist motion in different activities. Simulation results indicate that there is space for performance improvement over reports of existing devices. We have developed a coupled piezoelectric rotational harvester model with multiple design variables for future optimization. Preliminary experimental results of the one-beam prototype demonstrate an average power output of 3.8 μW in pseudo walking motion while improvement can be made by finishing the prototype with the full 6-beam assembly.

Future work will include the experimental validation of the full 6-beam prototype harvester, further optimization based on all the design variables of the coupled harvester model, and the incorporation of custom designed and fabricated piezoelectric elements.

6. Acknowledgement

The authors would like to thank the NSF Nanosystems Engineering Research Center (NERC) for Advanced Self-Powered Systems of Integrated Sensors and Technologies (ASSIST) for financial support as well as the UVA Center for Wireless Health for providing the wrist motion data.

References

[1] Yun J, Patel S N, Reynolds M S and Abowd G D 2011 *IEEE Trans. Mob. Comput.* **10** 669–83
[2] http://www.seikodigitalwatches.com/5XXX/5M6263A.pdf, Accessed October 2014.
[3] Pillatsch P, Yeatman E M and Holmes A S 2013 *J. Phys. Conf. Ser.* **476** 012010
[4] Rao Y, McEachern K M and Arnold D P 2013 *J. Phys. Conf. Ser.* **476** 012011
[5] Yeatman E M 2008 *Proc. Inst. Mech. Eng. Part C J. Mech. Eng. Sci.* **222** 27–36
[6] Mitcheson P D *et al.* 2008 *Proceedings of the IEEE* **96** 1457–86
[7] Halvorsen E Le C P Mitcheson P D and Yeatman E M 2013 *J. Phys. Conf. Ser.* **476** 012026
[8] Barth A T, Hanson M A, Powell H C and Lach J 2009 *The 6th International Workshop on Wearable and Implantable Body Sensor Networks* 71–76
[9] Erturk A and Inman D J 2008 *Journal of Vibration and Acoustics* **130** 1–15
[10] Pillatsch P, Yeatman E M and Holmes A S 2014 *Smart Materials and Structures* **23** 025009